CORRELATION OF MERCURY SPECTRAL UNITS WITH GEOLOGY AND ELEMENTAL ABUNDANCE. Noam R. Izenberg (noam.izenberg@jhuapl.edu)[1], Pegah Pashai[2], Mark C. Kochte[1], Rachel L. Klima[1], Shoshana Z. Weider[3], Larry R. Nittler[3], Richard D. Starr[4], Ellen J. Crapster-Pregont[5], Faith Vilas[6], and Sean C. Solomon[3,7]. [1]Johns Hopkins University Applied Physics Laboratory, Laurel, MD 20723, USA. [2]University of Maryland, College Park, MD 20742, USA. [3]Dept. of Terrestrial Magnetism, Carnegie Institution of Washington, Washington, DC 20015, USA. [4]The Catholic University of America, Washington, DC 20064, USA. [5]American Museum of Natural History, New York, NY 10024, USA. [6]Planetary Science Institute, 1700 E. Fort Lowell, Suite 106, Tucson AZ, 85719, USA. [7]Lamont-Doherty Earth Observatory, Columbia University, Palisades, NY 10964, USA.

Introduction: We use orbital data from the Mercury Surface and Atmospheric Composition Spectrometer (MASCS) Visible and Near Infrared Spectrograph (VIRS) [1] on the MErcury Surface, Space ENvironment, GEochemistry, and Ranging (MESSENGER) spacecraft to study subtle compositional variations across the surface of Mercury. Most of the surface is covered by plains units with brightness (represented here by reflectance at 575 nm; "R575") and spectral reflectance ratios (e.g., "VISr": 415 nm/750 nm and "UVr": 310 nm/390 nm) that vary within small ranges [2] (Fig. 1a) and can be divided into four spectral units on the basis of clustering in this parameter space [2]. This work represents a preliminary attempt to subdivide and refine these earlier groupings [2]. A preliminary spectral unit map of Mercury (Fig. 1b) covers ~90% of the planet.

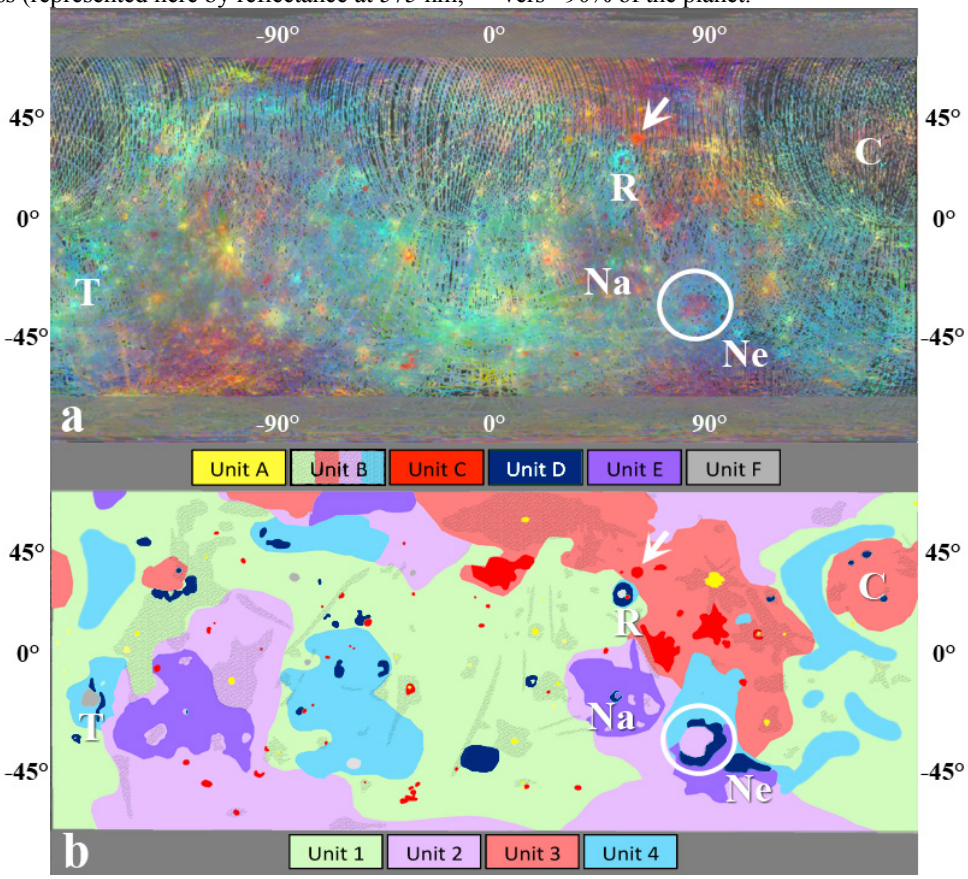

Fig. 1. VIRS maps of Mercury (dark grey regions are excluded from our analysis). (a) Color composite: Red = R575, green = VISr, blue = UVr. (b) Preliminary VIRS spectral unit map. Unit B shown as light gray shading on other units. Unit boundaries are gradational, not sharp. T = Tolstoj, R = Rachmaninoff, Na = Nabokov, Ne = Neruda, C = Caloris. Rembrandt basin is circled. Arrow points to pyroclastic deposit NE of Rachmaninoff.

Spectral Units: On the basis of reflectance and spectral ratios from VIRS and superposition relationships deduced from Mercury Dual Imaging System (MDIS) [3] color and high-resolution images, we have defined four "background" spectral map units (units 1–4) that collectively span much of the surface and six "regional" spectral units (units A–F) of smaller extent. The four background units are all subunits of the "average spectral unit" [2] and fall within the spectral parameter space of that unit. Unit 1 covers almost half of the mapped area and has reflectance and spectral ratio parameters within a few percent of planetary mean values. Units 2–4 each cover progressively less of the surface and have spectral parameter characteristics described qualitatively in terms of distance from mean values in Table 1. Units 2 and 3 together correspond partly, but not completely, to the polar spectral unit identified from unsupervised classification of VIRS data [4]. The regional units each have distinctive spectral characteristics

described in Table 1. The table also indicates how the spectral units adopted here relate to the four VIRS spectral units defined earlier [2].

Table 1. VIRS spectral units relative to average parameter values.

Unit	1	2	3	4	A	B	C	D	E	F
R575	-	↑	↑	↓	↑↑	↑	↑	↓	-	↓↓
VISr	-	↓	↓	↓	↑↑	↑	↓↓	-	↓↓	↓
UVr	-	-	↓	↑	↓	-	↓↓	↑↑	↑	↓
VSU	Average				Bright		Red	Dark Blue	Between units	

Parameter trends for units in Fig. 1. Values near Mercury mean have a dash. High values are denoted by upward arrows; low values are denoted by downward arrows. VSU = VIRS spectral unit [2].

Correlation with geology and MDIS color: Our background units were guided by visual interpretation of Fig 1a. When compared with morphological and color characteristics [5, 6], unit 1 is broadly associated with intermediate terrain [5] or lower-reflectance intercrater plains [6] and heavily cratered terrain. Units 2, 3, and 4 all cover portions of smooth plains [6] but are not restricted to that terrain. Unit 2 includes areas of smooth plains in the northern lowlands but also regions in the south and at mid-latitudes. Unit 3 includes some northern plains and Caloris interior plains (high-reflectance red plains, or HRP) [5], but also a mid-latitude region. Unit 4 generally coincides with low-reflectance blue plains (LBP), including the circum-Caloris plains [5,6]. Stratigraphically, only unit 3 appears consistently on top of the other background units that surround it.

The regional units tend to have characteristic geological associations. Unit A corresponds with fresh craters, crater floors, high-reflectance ejecta, and hollows [8, 9]. Unit B consists of older craters, extended crater ejecta, and crater rays. Units A and B fall in the parameter space of the bright spectral unit [2]. Unit C corresponds to the red spectral unit [2] and includes primarily pyroclastic deposits [8]. Unit D corresponds to the blue spectral unit [2] and includes low-reflectance material (LRM) [5], large crater rims/rings, and some crater rays [10]. Unit E is found in areas of high UVr (*e.g.,* the Nabokov and Neruda regions). Unit F is made up of small regions (e.g., floors of basins such as Tolstoj and Rachmaninoff) with lower than average reflectance, but are not LRM-like in other parameters. Stratigraphically, units A and B tend to overlie all other units. Unit C overlies most others. Units D, E, and F appear to overlie surrounding background units.

Correlation with elemental composition: Variations in spectral reflectance appear partially related to XRS-measured variations in elemental ratios [4,11], shown in Fig. 2. Areas of high S/Si ratio (Fig. 2a) appear to coincide with unit 4. Regions with the lowest S/Si ratio consist of units 3 and C; targeted XRS observations have documented low sulfur in the pyroclastic deposit near Rachmaninoff (unit C, arrow in Fig. 1a, b) [12]. The relationship of the spectral units to Ca is similar to that for S. Fe/Si ratio (Fig. 2b) is poorly correlated with the VIRS spectral units. Some high Fe regions appear to coincide with unit E, but this comparison is limited by the lack of high-spatial-resolution Fe data [13]. The Mg/Si ratio (Fig. 2c) is poorly correlated globally with the spectral units, but the high-Mg area of Rachmaninoff coincides spatially with an isolated region of unit 4, and the low-Mg Caloris interior smooth plains closely follow unit 3 in this area [14]. The biggest gaps that remain in the XRS Mg/Si map are mostly in unit 3 regions. XRS-derived Al content shows no spatial correlation with the VIRS spectral units.

Discussion: Units A, B, C are all higher in reflectance and correspond geologically with younger features such as fresh craters, hollows, and pyroclastic deposits. With the exception of unit C, these superposed regional units have less steeply sloped spectra than the background units. The lower reflectance and steeper spectral slope (low VISr) of the background units are probably related to the darkening, reddening, and homogenizing processes of space weathering [15]. On a global scale, VIRS spectral units show some relation to XRS observations for S, Ca, Fe, and Mg, but virtually none for Al [cf. 4]. The correlations between spectrally derived units and XRS elemental ratios suggest that subtle differences in the reflectance of Mercury's topmost surface can be affected by variations in elemental abundances.

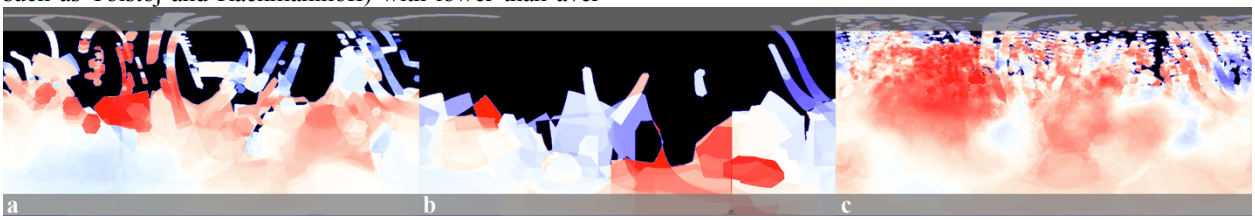

Fig. 2. XRS element ratio maps [12, 16] with colors stretched to emphasize highest ratio values (red) and lowest non-zero ratios (blue). (a) S/Si; maximum value = 0.16. (b) Fe/Si; maximum value = 0.09. (c) Mg/Si; maximum value = 0.91. Black areas are not yet mapped by XRS. The areas shown in each panel correspond to that in Fig. 1.

References: [1] McClintock W. E. and Lankton M. R. (2007) *Space Sci. Rev. 131*, 481–522. [2] Izenberg N. R. et al. (2014) *Icarus 228*, 364-374. [3] Hawkins S. E., III, et al. (2007) *Space Sci. Rev. 131*, 247–338. [4] D'Amore M. et al. (2014) *LPS 45,* this volume. [5] Denevi B. W. et al. (2009) *Science 324*, 613–618. [6] Denevi B. W. et al. (2013) *JGR Planets, 118*, 891–907. [7] Head J. W. et al. (2011) *Science 333*, 1853–1856. [8] Kerber L. et al. (2009) *Earth Planet. Sci. Lett. 285*, 263–271. [9] Blewett D. T. et al. (2011) *Science 333*, 1856–1859. [10] Robinson M. S. et al. (2008) *Science 321*, 66–69. [11] Izenberg N. I. et al. (2013) *LPS 44*, abstract 3018. [12] Nittler L. R. et al. (2014) *LPS 45*, this volume. [13] Weider S. Z. et al. (2014) *Icarus*, submitted. [14] Weider S. Z. et al. (2014) *LPS 45*, this volume. [15] Domingue D. L. et al. (2014) *LPS 45*, this volume. [16] Nittler L. R. et al. (2013) *LPS 44*, abstract 2458.